The Beagle, Records of the Museums and Art Galleries of the Northern Territory, 2000 **16**: 145-162

Two new genera and three new species of Thylacinidae (Marsupialia) from the Miocene of the Northern Territory, Australia

PETER MURRAY[1] AND DIRK MEGIRIAN[2]

[1]*Museum of Central Australia, PO Box 2108,*
Alice Springs, NT 0871, AUSTRALIA
peter.murray@nt.gov.au
[2]*Museum and Art Gallery of the Northern Territory, GPO Box 4646,*
Darwin, NT 0801, AUSTRALIA
dirk.megirian@nt.gov.au

ABSTRACT

Three new species and two new genera of Thylacinidae from the Northern Territory of Australia bring the total number of known mid and late Tertiary species to 11 in eight genera. *Tyarrpecinus rothi* gen. et sp. nov. from the Alcoota Local Fauna (Waite Formation), and *Nimbacinus richi* sp. nov. and *Mutpuracinus archibaldi* gen. et sp. nov. from the Bullock Creek Local Fauna (Camfield Beds), are relatively small and amongst the more plesiomorphic members of the family. Phylogeny reconstruction using cladistic methods and biochronological data indicate that a major radiation occurred within the family in pre-Miocene times. Specialisation in the form of dental carnassialisation appears to have evolved in parallel in at least two crown groups, one of which includes the recently extinct 'Tasmanian wolf', *Thylacinus cynocephalus*. The other, together with all the lineages represented by unspecialised species, apparently did not survive into the late Miocene. However, insufficient data are available to show what the regional, let alone continental, pattern of succession was during the Miocene.

KEYWORDS. Marsupialia, Thylacinidae, *Mutpuracinus archibaldi* gen. et sp. nov., *Tyarrpecinus rothi* gen. et sp. nov., *Nimbacinus richi* sp. nov., Alcoota Local Fauna, Bullock Creek Local Fauna, Camfield Beds, Waite Formation, phylogeny, evolution, Miocene, Australia.

INTRODUCTION

The Thylacinidae is a family of dasyuromorphian marsupials, the last member of which, the Tasmanian wolf (*Thylacinus cynocephalus* (Harris)), was extinguished by bounty hunters in the 1930s. Pliocene and Pleistocene fossil species have all been synonymised with *T. cynocephalus* (Dawson 1982), and the fossil record of the family was only extended into the late Miocene with the discovery at Alcoota of *Thylacinus potens* Woodburne, 1967. *Thylacinus potens* provided the first indication that thylacinids were a radiated family, as the species is derived dentally in ways that precludes its direct ancestry of *T. cynocephalus*. In more recent years, the fossil record has been greatly expanded by new discoveries at Alcoota, Bullock Creek and Riversleigh (Fig. 1), spanning the ?late Oligocene to late Miocene (Muirhead and Archer 1990; Wroe 1996; Muirhead 1997; Murray 1997; Muirhead and Wroe 1998). On the basis of the known diversity of thylacinids in the central and northern Australian deposits, it might be anticipated that similar diversity will eventually be found in correlative deposits in the Lake Eyre and Tarkarooloo Basins of South Australia. So far, only a single premolar of unknown affinity has been listed from Lake Ngapakaldi, South Australia (Kutjamarpu Local Fauna, Wipijiri Formation of the Lake Eyre Basin) (Archer 1982). Hypotheses of phylogeny within the family are currently in a state of flux as each new discovery adds to the diversity of fossil forms available for analysis.

Tyarrpecinus rothi gen. et sp. nov. (Alcoota LF, late Miocene), *Mutpuracinus archibaldi* gen. et sp. nov. and *Nimbacinus richi* sp. nov. (both Bullock Creek LF, mid Miocene) represent three new species and two new genera of Thylacinidae, and raise the total number of known Tertiary species to 11 in eight genera. The new species are comparatively small members of the family (small and medium-dog sized, compared to the wolf-sized *T. cynocephalus*, for example). Cladistic analysis of dental characters resolves them as plesiomorphic members of the family, closely related to certain previously described forms (Muirhead 1992, 1997; Wroe 1996; Muirhead and Wroe 1998). Excellent preservation of the maxilla of *Mutpuracinus* and a complete dentary of *Nimbacinus richi* sp. nov. fill some important gaps in

Fig. 1. ?Late Oligocene and Miocene localities that have produced thylacines.

our knowledge of Tertiary thylacinid morphology. The three new species and other recently reported late Oligocene and Miocene finds exemplify a gradual structural succession towards the genus *Thylacinus*.

The current consensus is that thylacinids are dasyuromorphians derived from a dasyurid ancestor, although a possible affinity with South American borhyaenoids was a matter of prolonged debate from 1903 into the 1980s (e.g. references in Archer 1982; Muirhead and Wroe 1998). We accept argument presented by Wroe (1996) and Muirhead and Wroe (1998) for the inclusion of *Muribacinus gadiyuli* Wroe, 1996, and *Badjcinus turnbulli* Muirhead and Wroe, 1998, in the Thylacinidae (rather than in the Dasyuridae), and offer no additional observations on the issue regarding the thylacinid status of the similarly plesiomorphic *Mutpuracinus archibaldi* gen. et sp. nov. Other than to remark on the assumption that the metaconid reduces uniformly along the tooth row in thylacinids, we support the re-diagnosis of the family presented in Muirhead and Wroe (1998).

METHODS

Adult dental terminology (Flower-Luckett) recognises P1-3, M1-4 (Flower 1869, Luckett 1993); all Archer (1978, 1982) terminology in cited literature has been converted. Specimens are Northern Territory Museum (NTM) Palaeontological collection unless designated QMF (Queensland Museum, Fossil collection). The thylacinid-producing formations referred to are not precisely dated, and their ages can at present only be loosely expressed in terms of the standard geological timescale. Consequently, modifiers such as 'early' and 'late' are left uncapitalised when attached to the standard Tertiary epochs so as not to imply a geochronological precision that does not exist. Stage-of-evolution biochronological concepts and terminology follow Megirian (1994).

Key to anatomical abbreviations.

A-E	Stylar cusps
AC	Anterior cingulum or precingulum
ALV	Alveolus
ANP	Angular process
CCR	Centrocrista
CON	Condyle
CRN	Reception notch for canine
END	Entoconid
HLD	Hypoconulid
HYD	Hypoconid
IFO	Incisive foramen
IOF	Infraorbital foramen
MAF	Mandibular foramen
MCL	Metaconule
MCR	Submasseteric crest
MEC	Metacone
MED	Metaconid
MEF	Mental foramen
MFO	Masseteric fossa
MJS	Maxillo-jugal suture
PAC	Paracone
PAD	Paraconid
PAF	Palatal fenestra
PCD	Precingulid
PCL	Protoconule
PMF	Posterior mental foramen
PMS	Premaxillo-maxillary suture
PRC	Protocone
PRD	Protoconid
PSD	Parastylid

SYSTEMATIC PALAEONTOLOGY

Order Dasyuromorphia Gill, 1872
Superfamily Dasyuroidea Goldfuss, 1820
Family Thylacinidae Bonaparte, 1838
Mutpuracinus gen. nov.

Type species. *Mutpuracinus archibaldi* sp. nov. by monotypy.

Diagnosis. Small thylacinid with strong expression of stylar cusps on M^{1-3}; large, posteriorly directed P^3; infraorbital foramen not in contact with jugal and situated over posterior root of M^1. Size similar to holotype of *Muribacinus gadiyuli* (QMF30386); lower position of zygomatic root, more anterior position of infraorbital foramen relative to the teeth (i.e. over anterior root of M^1); more posteriorly-directed premolar crowns; larger posterolingual cuspule on P^3; M^2 narrower relative to length; larger stylar cusp D on M^{1-3} and

presence of stylar cusp C and E on M^{1-2}; paracone more reduced relative to metacone on M^{1-2}; M_4 metaconid more reduced; narrower cingulids and talonids on lower molars. Differs from *Badjcinus turnbulli* in which the jugal closely approaches the infraorbital foramen opening above P^3; the upper premolar crowns are more slender, taller; M^1 lacks stylar cusps on anterior lobe, preparacrista parallel to long axis of tooth row and M^3 with minute stylar cusp D. Differs from *Nimbacinus dicksoni* Muirhead and Archer, 1990, which is significantly larger; the infraorbital foramen is within the jugal and situated over anterior root of M^2; in which conules are more strongly expressed and M^2 distinctly longer than M^3. Differs from *Wabulacinus ridei* Muirhead, 1997, *Ngamalacinus timmulvaneyi* Muirhead, 1997, and species of *Thylacinus* in showing less reduction of metaconids on M_{2-4}; absence of carnassial notch in cristid obliqua and less reduction of entoconid and protocone.

Etymology. *Mutpura* is the tribal designation of the Aboriginal people living in the Camfield district [= *Tjambutjambulani* - Tindale 1974] + *kynos* (Gr.) 'dog'.

Mutpuracinus archibaldi sp. nov.

(Figs 2-4, Table 1)

Diagnosis. As for genus.

Type material. HOLOTYPE - NTM P907-3 (Blast Site), left maxilla with P^2-M^4, missing canine and P^1. PARATYPE - NTM P9612-5 (Top Site), left dentary fragment with M_{3-4}, missing ascending ramus and anterior part of horizontal ramus.

Referred material. All NTM: P9464-120 (Top Site), right premaxilla with I^{1-4} alveoli; P9464-119 (Top Site) posterior fragment of horizontal ramus of right dentary preserving submasseteric crest, part of condyle and part of angular process; P87108-10 (Blast Site), isolated right M_4.

Type locality. 'Blast Site', Bullock Creek, Northern Territory, Australia. Low limestone hill 1 km east of type section of Camfield Beds; 131° 31'E, 17° 07'S; Wave Hill 1:250 000 Map Sheet, SE/52-8.

Lithic unit, fauna and age. Camfield Beds, Bullock Creek Local Fauna, middle Miocene on the basis of marsupial stage-of-evolution biochronology (Woodburne *et al.* 1985; Murray *et al.* 2000). Both fossil quarries (sites) listed above are in the vicinity of the type locality (Murray and Megirian 1992: fig. 2).

Description. *Premaxilla* (Fig. 2A,B). Edentulous, 13.0 mm anteroposteriorly by 11.5 mm dorsoventrally, right premaxillary fragment P9464-120 is missing the ascending process. Four incisor alveoli are present: I^1 is largest; I^{2-3} are narrower; and I^4 is slightly smaller than I^1 but larger than I^{2-3}. The incisor arcade is nearly straight and less acutely angled relative to the midline than in *Dasyurus hallucatus* (Dasyuridae), for example. A large reception socket for the lower canine measures 4.5 mm anteroposteriorly by 6.5 mm dorsoventrally. The anterior margin of the right incisive foramen indicates a narrow, slot-like structure.

Maxilla (Fig. 3A,B). P907-3 preserves alveoli for

Table 1. Measurements (mm) of cheek teeth. L= length; W = width; AW = anterior width; PW = posterior width.

***Mutpuracinus archibaldi* gen. et sp. nov.**									**lower cheek teeth**											
	P_1		**P_2**		**P_3**				**M_1**			**M_2**			**M_3**			**M_4**		
	L	W	L	PW	L	AW	PW		L	AW	PW	L	AW	PW	L	AW	PW	L	AW	PW
P9612-5	-	-	-	-	-	-	-		-	-	-	-	-	-	5.7	3.6	2.9	5.9	3.3	2.3
P87108-10	-	-	-	-	-	-	-		-	-	-	-	-	-	-	-	-	5.3	2.9	2.2
									upper cheek teeth											
	P^1		**P^2**		**P^3**				**M^1**			**M^2**			**M^3**			**M^4**		
	L	W	L	PW	L	AW	PW		L	AW	PW	L	AW	PW	L	AW	PW	L	AW	PW
P907-3	-	-	4.5	1.8	5.5	2.4	3.0		5.8	4.1	6.2	5.7	5.0	6.5	5.4	5.7	7.0	6.0	4.7	3.5

***Nimbacinus richi* sp. nov.**									**lower cheek teeth**											
	P_1		**P_2**		**P_3**				**M_1**			**M_2**			**M_3**			**M_4**		
	L	W	L	PW	L	AW	PW		L	AW	PW	L	AW	PW	L	AW	PW	L	AW	PW
P9612-4	5.0	2.0	6.1	2.8	7.2	2.1	3.1		7.0	3.3	4.2	8.3	4.5	4.4	8.2	5.0	4.0	8.7	4.2	2.5
P8695-92	-	-	5.8	2.8	-	-	-		6.2	2.9	3.2	-	-	-	-	4.3	3.6	7.2	-	3.0
P904-7	-	-	-	-	-	-	-		-	-	-	7.4	4.1	4.3	8.0	4.5	4.1	7.9	4.1	2.9
P85553-3	4.5	1.7	6.0	2.8	-	-	-		6.9	-	4.0	-	-	-	-	-	-	-	-	-

***Tyarrpecinus rothi* gen. et sp. nov.**									**upper cheek teeth**											
	P^1		**P^2**		**P^3**				**M^1**			**M^2**			**M^3**			**M^4**		
	L	W	L	PW	L	AW	PW		L	AW	PW	L	AW	PW	L	AW	PW	L	AW	PW
P98211	-	-	6.5	2.5	-	-	-		4.8	7.0	7.3	-	-	-	7.7	7.9	9.8	-	-	-

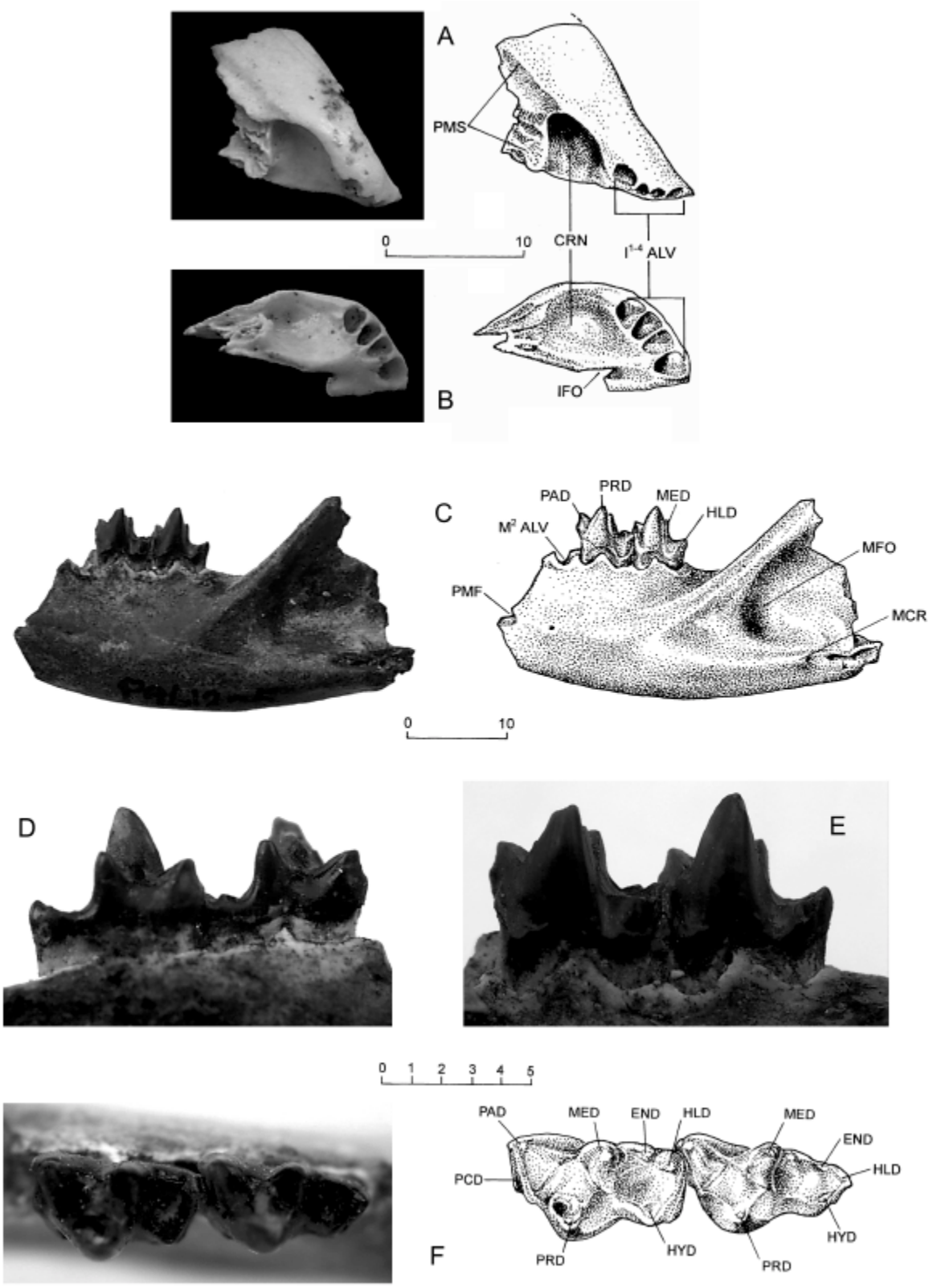

Fig. 2. *Mutpuracinus archibaldi* gen. et sp. nov. Referred right premaxilla (P9464-120) in **A**, lateral, and **B**, occlusal views. Paratype left dentary fragment (P9612-5) in **C**, lateral view; **D**, medial, **E**, lateral and **F**, occlusal, views of molars M_{3-4}. Scale bars in mm.

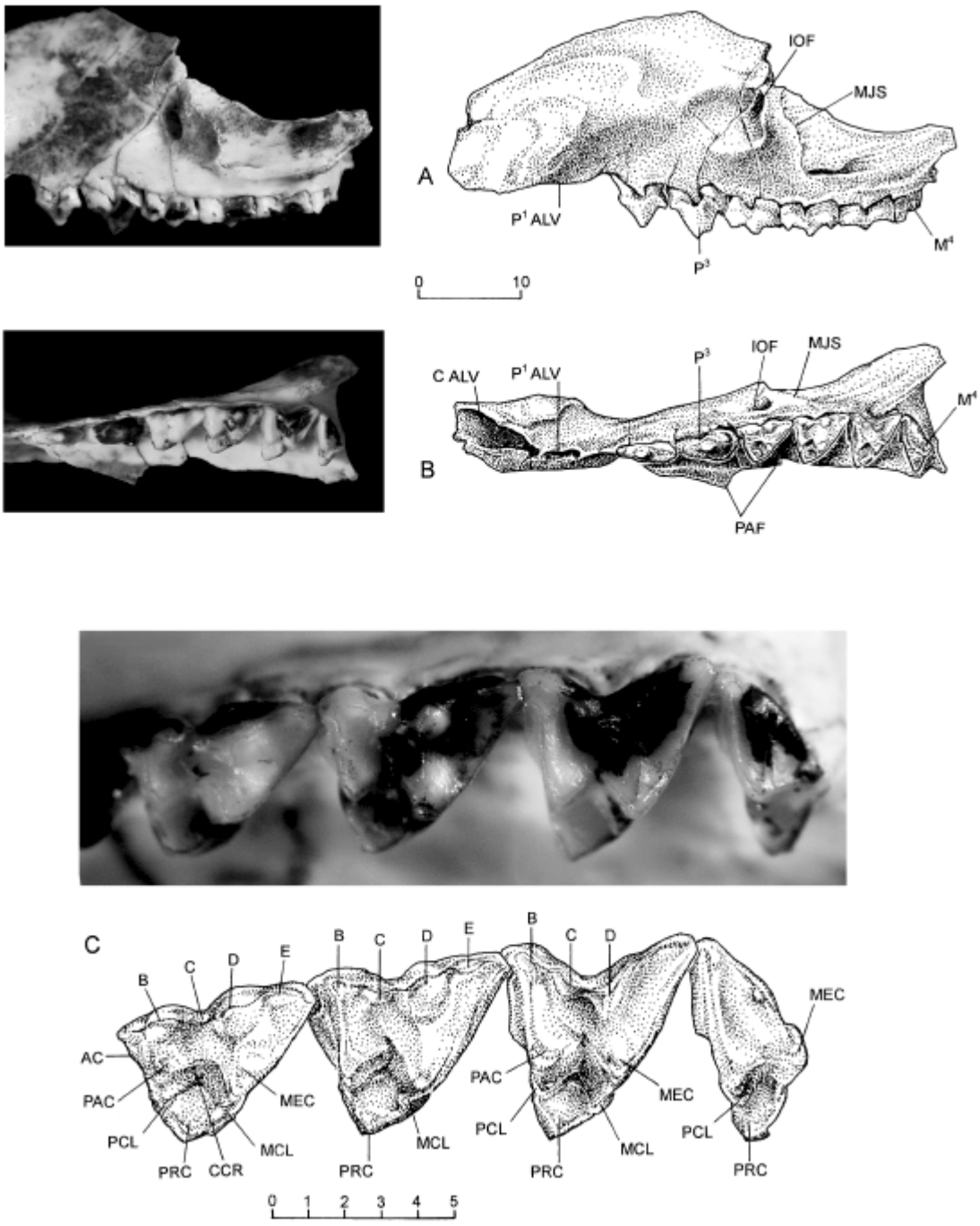

Fig. 3. *Mutpuracinus archibaldi* gen. et sp. nov. holotype left maxilla (P907-3) in: **A**, lateral view; **B**, occlusal view; and **C**, detailed occlusal view of molars M^{1-4}. Scale bars in mm.

upper canine and P^1 and remainder of left cheek tooth row; premaxillary contact preserved anterodorsally and nasal contact preserved dorsally; posterior (lacrimal) process missing; jugal process intact. Canine alveolus planoconvex, about 3.5 mm wide by 5.5 mm antero-posteriorly. Alveolus for P^1 situated immediately posterior to the canine alveolus, about 3.5 mm long, oriented slightly obliquely to succeeding premolars. A diastema 4.0 mm long separates P^1 from P^2. Crown of P^2 4.6 mm long, separated from P^3 by narrow, but distinct, slot that, while only 0.7 mm wide, is suggestive of rudimentary diastema. P^3 much larger than P^2 with crown projecting well below occlusal line of the other cheek teeth. Labial margin of molar row gently arcuate. Interdental embrasures present between M^{1-3}, becoming increasingly larger and distinct posteriorly. Anterior margin of posterior palatal fenestra preserved at the level of P^3/M^1. Palatal processes thin posteriorly, thickening anteriorly in front of fenestral margin towards P^3. Jugal contact a shallow, crescentic depression extending to

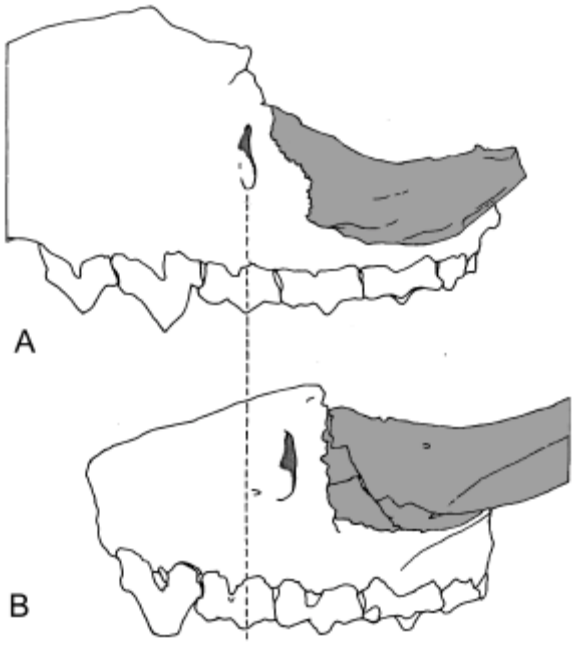

Fig. 4. Comparison of maxillae of **A**, *Mutpuracinus archibaldi* gen. et sp. nov. and **B**, *Muribacinus gadiyuli* drawn to the same scale, showing differences in the position of the infraorbital foramen relative to M^1. (B reversed: after Wroe 1996: fig. 1.)

within about 2.5 mm of infraorbital foramen dorsally and about 4.0 mm ventrally. Infraorbital foramen large, about 5.0 mm vertically and 2.5 mm mediolaterally (Fig. 4), opening behind well-defined circular infraorbital fossa, about 12 mm in diameter. The posterior margin of the foramen is aligned with the distal root of M^1. A shallow depression extending anterodorsally from infraorbital fossa is bounded dorsally by very distinct, sinuous groove terminating about 12 mm above level of canine alveolus. External surface of the canine alveolus bulges conspicuously outwards from surrounding contours of maxilla, resulting in a wide concavity in the vertical profile of specimen. Lateral surface of alveolar bulge rugose, with sharply defined posterior crest.

Incisors, I^{1-4}. Alveoli only (Fig. 2A,B): I^1 largest, broadly oval, 2.0 mm wide, 2.1 mm anteroposteriorly; I^2 triangular, 1.5 mm wide, 1.8 mm long, slightly wider than I^3; I^3 narrow, slot-like; 1.3 mm wide, 2.1 mm long; I^4, ovo-triangular, 1.8 mm wide, 2.0 mm anteroposteriorly.

Canine. Alveolus only (Fig. 2A,B), 5.5 mm anteroposteriorly; 3.5 mm mediolaterally; planoconvex shape; root socket 14.0 mm deep, angled ~30° to palatal plane.

Premolar, P^1 (Fig. 3A,B). Alveolus only, 3.5 mm anteroposteriorly, anterior root socket 1.3 mm diameter; angled about 12° from plane of P^{2-3}.

P^2 (Fig. 3A,B). Crown 4.5 mm long, 1.8 mm maximum width; low anterior basal crest, concave anterior margin, tip directed posteriorly; slight posterolingual expansion and small posterobasal cuspule; posterior root larger than anterior.

P^3 (Fig. 3A,B). Much larger than P^2, 5.5 mm anteroposteriorly by 3.0 mm posterior width; low anterobasal crest; concave, rounded anterior margin, tip directed posteriorly; convex, crested posterior margin; low, well-developed posterolingual cuspule developed on thick basal cingulum, terminating in elevated posteromedian cuspule; posterolabial cingulum poorly developed.

Molar, M^1 (Fig. 3C). Paracone situated much more labially than metacone, very short transverse preparacrista; centrocrista nearly parallel to axis of tooth row; metacone large, premetacrista nearly transverse. Talon broad anteroposteriorly and short transversely; small metaconule and protoconule present; protocone large. Stylar cusp B closely adpressed to paracone; higher but slightly smaller than the latter; vestigial stylar cusp C situated at base of stylar cusp D, a large conical cuspule occupying about half the posterior lobe of the crown. Well-developed ectoflexus present, buccal occlusal profile of crown distinctly lobate. Low swelling in the position of stylar cusp E (heavily worn); weak precingulum present with shallow interproximal notch for P^3.

M^2 (Fig. 3C). Larger, more equi-triangular crown; paracone extends much further lingually than in M^1; short, transverse preparacrista extends to stylar cusp B; stylar cusp C well-developed, about equal in size to B; stylar cusp D large, conical, occupies slightly less than half of metastylar lobe of crown, slightly smaller but nearly equal in height to metacone; small, distinct stylar cusp E situated midway between D and metastylar tip. Metacone much larger than paracone. Talon broad, but more V-shaped than in M^1, conules small, protocone narrow. Precingulum well-developed with notch for metastyle of M^1.

M^3 (Fig. 3C). Larger than M^2 in occlusal aspect, significantly wider transversely, equal in length labially and slightly longer posterolingually; stylar cusp B reduced; stylar cusp C well-developed but low; stylar cusp D large, triangular, but considerably reduced in height and transverse width; tiny cuspule present in position of stylar cusp E. Ectoflexus strong, parastylar and metastylar tips slender, lobate. Preparacrista long, straight, transverse; paracone less reduced relative to metacone; postmetacrista longer than in M^2. Talon narrow, distinctly V-shaped, small conules present, more distinct than in M^2; protocone reduced. Precingulum longer than in M^2 with V-shaped accommodation notch for M^2 metastyle.

M^4 (Fig. 3C). Tip of parastyle situated lingual to tip of M^3 metastyle; preparacrista slightly convex, about equal in length to M^3; metacone greatly reduced, Protoconule better developed than on other molars; metaconule absent; talon narrow; preprotocrista weak. A tiny stylar cusp is situated midway between parastylar tip and base of metacone.

Meristic gradients, M^{1-4} (Fig. 3C). Preparacrista:

increases posteriorly, M^{3-4} about equal; postmetacrista: increases posteriorly except M^4 where absent; paracone height: increases posteriorly M^{1-3}, M^4 equals or slightly lower than M^3; metacone height: increases posteriorly, except M^4 where reduced; protocone height: decreases posteriorly; talon surface: increases posteriorly M^{1-2}, decreases posteriorly M^{3-4}; stylar cusp B size: decreases M^{1-4}; stylar cusp C: increases M^{1-3}, absent M^4; stylar cusp D: decreases M^{1-3}, absent M^4; stylar cusp E: decreases M^{1-2}, possibly M^3, absent M^4.

Dentary (Fig. 2C). Medial surface flat, digastric fossa faint, shallow; subalveolar fossa, lateral crest well-defined. Masseteric fossa deep with prominent shelf-like submasseteric crest. Depth of horizontal ramus below M_4 14.0 mm; thickness of inferior border at same level, 5.5 mm.

M_3 (Fig. 2C-F). Paraconid and protoconid bulky; metacristid nearly perpendicular to long axis of crown; talonid distinctly narrower than trigonid; metaconid large, higher than paraconid, bulky at base. Entoconid small but distinct; as high as hypoconulid; hypoconulid merges labially with postcingulid. Hypoconid lowest cusp on crown; pre- and postcingulids present but not strongly developed. Cusp heights: protoconid> metaconid> paraconid> entoconid= hypoconulid> hypoconid.

M_4 (Fig. 2C-F). Cusps of trigonid more slender, talonid greatly reduced compared to M_3; metaconid and paraconid similar in height to M_3 but more slender. Entoconid reduced to thickening of preentocristid, lower than hypoconulid; hypoconulid high pointed cusp, continuous labially with postcingulid. Pre- and postcingulids not strongly developed. Cusp heights: protoconid> metaconid> paraconid> hypoconulid> entoconid> hypoconid.

Meristic gradients M_{3-4} (Fig. 2C-F). protoconid, paraconid and metaconid decrease in bulk posteriorly; talonid decreases in width posteriorly; entoconid decreases in size posteriorly; angle of paracristid to long axis of crown more acute posteriorly.

Etymology. Named after Ian Archibald in honour of his contributions to the natural history of the Northern Territory.

Nimbacinus Muirhead and Archer, 1990

Type species. *Nimbacinus dicksoni* Muirhead and Archer, 1990, by original designation.

Nimbacinus richi sp. nov.

(Fig. 5, Table 1)

Nimbacinus dicksoni - Muirhead and Archer 1990: fig. 3 (in part).

Diagnosis. Medium-sized thylacinid with narrow diastemata between premolars, P_3 much larger than P_2; lower molars with well-developed metaconids and entoconids. Differs from *Nimbacinus dicksoni* in possessing well-developed metaconids on M_{2-4} in conjunction with reduced metaconid on M_1 and large conical entoconids on M_{1-3}; differs from *Ngamalacinus timmulvaneyi* and *Badjcinus turnbulli* in lacking a carnassial notch in the hypocristid, and from *Wabulacinus ridei* Muirhead, 1997, and species of *Thylacinus* in having large metaconids.

Type material. HOLOTYPE - NTM P9612-4 (Top Site), right dentary with P_1-M_4; canine, incisors missing. PARATYPE - NTM P85553-3 (unrecorded quarry), fragment of right dentary with P_{1-2} and M_1 (also a paratype of *N. dicksoni* Muirhead and Archer, 1990).

Type locality. 'Top Site', Bullock Creek, Northern Territory (additional data as for *Mutpuracinus archibaldi*).

Referred material. NTM P8695-92 (Blast Site), horizontal ramus of left dentary retaining P_2, M_1, M_{3-4} (M_3 lacking paraconid); P904-7 (Top Site), left dentary fragment retaining M_{2-4}.

Lithic unit, fauna and age. Camfield Beds, Bullock Creek Local Fauna, mid Miocene (additional information as for *Mutpuracinus archibaldi*).

Description. *Dentary* (Fig. 5A,B). P9612-4 is about 25% smaller than *Thylacinus macknessi* Muirhead, 1992, but relatively stouter anteriorly and more bowed along inferior border; anterior margin of ascending ramus more erect, condylar notch wider, more invasive. Diastema between P_2-P_3 very short, approximately 1.4 mm; large mental foramen under posterior root of P_1, small posterior mental foramen under posterior root of M_1. Masseteric crest well developed, flange-like; masseteric fossa relatively shallower and condyle; condyle transversely elongate (14.0 mm wide), slightly flattened dorsally. Mandibular foramen situated 22.0 mm from distal edge of condyle; depth of ramus below M_4 is 15.6 mm; thickness of inferior border at same level is 7.0 mm.

Incisors, I_{1-3} (Fig. 5A,B). Three incisor alveoli present anteromedial to canine alveolus, arranged in a triangle, I_3 ventrolaterally, I_2 lingually and I_1 above I_2 but aligned vertically with I_3; I_3 socket smallest (1.3 mm x 1.5 mm) followed by I_2 (1.3 mm x 2.5 mm) with I_1 largest (1.5 mm x 3.0mm); lateral width of all three sockets about 3 mm, vertical extent about 4.8 mm.

Canine (Fig. 5A,B). Alveolus only (7.4 mm vertical, 4.0 mm mediolateral) oval socket, anterolaterally directed.

Premolars, P_{1-3} (Fig. 5A,B). P_1 oriented obliquely (approximately 15°) to long axis of other premolars, much smaller than P_2 (5.0 mm long, 2.0 mm wide) with low, recurved protoconid and very elongated posterior shelf lacking distinct cuspule. Protoconid of P_2 much higher, longer than P_1; small anterobasal and posterobasal cuspules present (6.1 mm long, 2.8 mm wide); P_3, anterobasal cuspule more defined, posterior shelf more talonid-like and elevated distally with small posterolingual and large posterobasal cuspules (7.2 mm

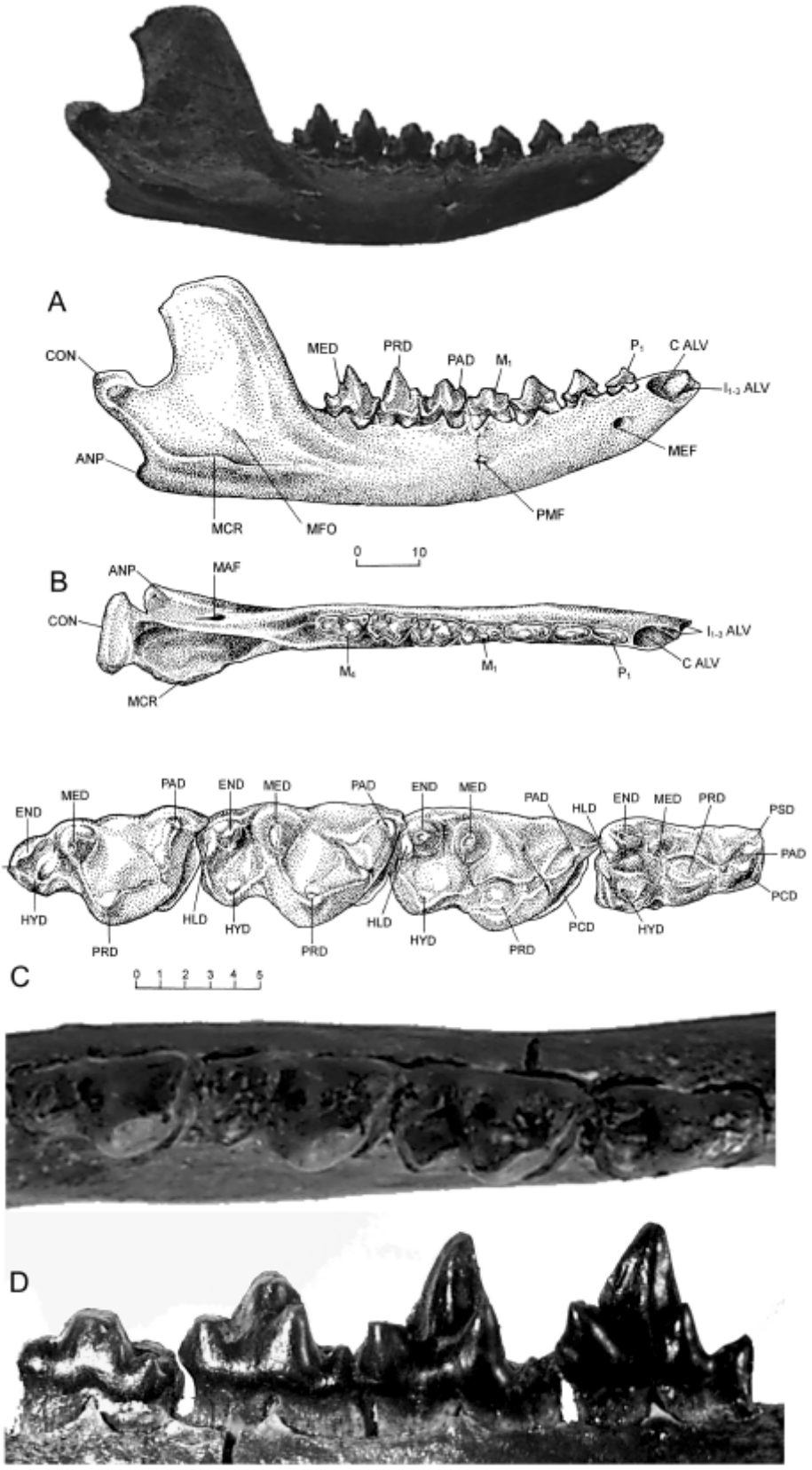

Fig. 5. *Nimbacinus richi* sp. nov. holotype right dentary (P9612-4) in: **A**, lateral view; **B**, occlusal view; **C**, molars M_{1-4} in occlusal view; and **D**, molars M_{1-4} in lateral view.

long, 3.1 mm wide). Protoconids of all premolars directed posteriorly.

Molar, M_1 (Fig. 5A-D). Subrectangular crown, rather truncated anteriorly and markedly so posteriorly; talonid wider than trigonid; short paracristid slightly angled lingually, paraconid low, broad, conical with short preparacristid terminating in small parastylid; protoconid central, crown shallowly waisted on either side; posterolingual corner of talonid forming right angle; entoconid prominent, posteriorly-directed, conical cusp about 1.5 mm in diameter, separated from base of metaconid by deep, transverse groove; entoconid much larger and higher than hypoconulid; hypoconid large, triangular, lowest cusp on talonid. Small metaconid represented by low, broad triangular bulge on posterolingual side of protoconid. Pre- and postcingulids thick, well developed anterolabially, terminating above middle of anterior root; postcingulid ascends to just below hypoconulid. Cusp heights: protoconid > metaconid > entoconid > paraconid > hypoconulid = hypoconid.

M_2 (Fig. 5A-D). Trigonid somewhat compressed, much longer and slightly wider than talonid; paracristid slightly less obtuse than in M_1; metaconid much larger and more differentiated from protoconid; small carnassial notch present in metacristid; entoconid slightly larger and higher than in M_1; extending high above smaller, flat, triangular hypoconulid and closely adpressed to parastylid of M_3. A short preentocristid developed. Hypoconulid extending distolabially a short distance beyond the entoconid where it is accommodated by distinct C-shaped notch between precingulid and parastylid. Hypoconid a broad, triangular cusp much lower than hypoconulid. Cristid obliqua ascending base of protoconid for short distance. Cusp heights: protoconid > metaconid > paraconid > entoconid > hypoconulid > hypoconid.

M_3 (Fig. 5A-D). Protoconid more slender than in M_2, paraconid higher, slightly more erect, metaconid also higher, more differentiated, but more slender than in preceding molar; talonid shorter and narrower relative to trigonid than in M_2. Entoconid reduced to small spur-like cusp on anterolingual margin of enlarged, triangular hypoconulid; hypoconulid projects distally into accommodation notch in M_4. Postcingulid reaches labial side of hypoconulid; hypoconid situated much lower than in M_2 and considerably reduced; cristid obliqua ascends posterior face of protoconid about halfway up to carnassial notch. Cusp heights: protoconid > metaconid > paraconid > hypoconulid > entoconid > hypoconid.

M_4 (Fig. 5A-D). Paraconid directed slightly more to lingual side than in M_3; para- and metacristids blade-like, with deep carnassial notches; metaconid greatly reduced though fully differentiated from protoconid; talonid width about half that of preceding molar; entoconid reduced to thickening of the preentocristid, hypoconulid formed as in preceding molar, but smaller, succeeded anteriorly by strong posthypocristid; postcingulid vestigial. Hypoconid small, situated low on posterolabial margin of talonid basin; talonid basin open labially; cristid obliqua strongly developed, ascends posterior face of protoconid to base of carnassial notch in metacristid. Cusp heights: protoconid > paraconid > metaconid > hypoconulid > entoconid > hypoconid.

Meristic gradients, M_{1-4} (Fig. 5A-D). Protoconid decreases in bulk posteriorly; paraconid increases in height and obliquity to long axis of crown posteriorly; metaconid increases markedly in bulk from M_1 to M_2 then gradually decreases; metaconid gradually increases in height to M_3 then decreases in M_4; entoconid increases in size and height to M_2 then decreases M_3 to M_4; hypoconulid increases in height posteriorly; hypoconulid increases in size posteriorly to M_3 then decreases in M_4; talonid increases in width from M_1 to M_2 then decreases from M_3 to M_4.

Remarks. Association of referred specimens of lower molars with the uppers in *Nimbacinus dicksoni* was problematic (Muirhead and Archer 1990). Muirhead and Archer (1990) note several differences between the holotype M_1 (QMF16802, 'Henk's Hollow', Carl Creek Limestone) and the Bullock Creek Local Fauna specimen (P85553-3). The latter specimen shows a stronger entocristid and a more angular posterolingual corner, resulting in greater posterior crown width and a more rounded contour of the anterolingual surface. Although very worn, the entoconid of P85553-3 (difficult to see in their illustration) is somewhat larger and more distinct than that of the holotype. The same differences are more emphasised in less-worn P9612-4 in which a large, conical entoconid is present. These distinctions appear to be consistent and therefore not readily attributable to individual variation. More important however, is the status of paratype QMF16809 (Site D locality), identified as a right M_2 (their M_3 in Archer (1978, 1982) terminology). If this specimen, that has a greatly reduced metaconid, represents *N. dicksoni* (as they argue at some length), then P9612-4, which has a large metaconid on M_2, could not represent this species. While a species-level distinction could be made on the basis of this technicality alone, the subsequent discovery of several similar-sized thylacinid species increases the probability that QMF16809 might not represent *N. dicksoni*, and therefore a systematic distinction made on this basis could be phylogenetically misleading. While the differences in M_1 morphology alone are sufficient to indicate the existence of another species of the genus *Nimbacinus*, this proposed revision leaves the states of the M_{2-4} metaconids of *N. dicksoni* in doubt.

Etymology. Named in honour of Thomas Rich for his many important contributions to vertebrate palaeontology in Australia. Tom introduced us to the Bullock Creek Local Fauna of the Northern Territory in 1984.

Tyarrpecinus gen. nov.

Type species. *Tyarrpecinus rothi* sp. nov. by monotypy.

Diagnosis. Medium-sized thylacinid with transversely narrow, elongate M^1 and strong ectoflex and elongation of metastylar spur on M^3; differs from *Muribacinus gadiyuli* and *Mutpuracinus archibaldi* in larger size, narrower M^1, more elongate and slender metastylar wing; wider angle between preparacrista and postmetacrista; more closely approximated paracone and metacone on M^3; differs from *Badjcinus turnbulli* in form of premolar crown; in possessing stylar cusps and preparacrista on the anterior lobe of M^1; more reduced stylar cusp B and relatively larger stylar cusp D on M^3; differs from *Nimbacinus dicksoni* and *Ngamalacinus timmulvaneyi* in having a more slender, elongated M^1 with straighter centrocrista and more reduced parastylar spur; M^3 metastylar spur more elongate; narrower trigone basin, metacone larger relative to paracone; conules where present, extremely reduced; differs from *Wabulacinus ridei* in more transverse orientation of preparacrista and retention of stylar cusps B and D on M^1; differs from *Thylacinus macknessi* in reduction of precingulum but retention of stylar shelf, otherwise showing conservative *Thylacinus*-like apomorphies.

Etymology. Eastern Arrente dialect *tyarrpa* 'cracked' + *Kynos* (Gr.) 'dog'. *Tyarrpa,* pronounced char-puh, (Henderson and Dobson 1994), is in reference to the state of preservation of the type material.

Tyarrpecinus rothi sp. nov.

(Fig. 6, Table 1)

Diagnosis. As for genus.

Type material. HOLOTYPE - NTM P98211 (Main Pit), fragment of left maxilla with P^2, M^{1-4}; M^1 and M^3 complete but assembled from fragments; M^2 and M^4 represented by talons only; approximately 75 small fragments consisting of isolated roots and bone and enamel fragments.

Type locality. Alcoota Scientific Reserve, Northern Territory, Australia. 22°52' S, 134°52' E; Alcoota 1:250,000 Map Sheet, SF/53-10.

Lithic unit, fauna and age. Waite Formation, Alcoota Local Fauna, late Miocene on the basis of marsupial stage-of-evolution biochronology (Woodburne *et al.* 1985; Murray *et al.* 1993, Murray *et al.* 2000).

Description. The *Tyarrpecinus rothi* sp. nov. holotype, P98211, was reconstituted from a concentration of small fragments of bone and teeth that may represent the contents of a crocodilian coprolite. Many of the fragments show chemical erosion and are coated with a layer of calcite. Part of the left maxilla has been assembled and, except for some conspicuous cracks and a few missing chips of enamel, the M^1 and the M^3 have been adequately restored for description.

Maxilla. Maxilla contains P^2 and anterior alveolus of P^3. A 4.5 mm long section of the diastema anterior to P^2 does not reach the P^1 alveolus. Palatal process extends to median palatal suture and is about 7.0 mm wide immediately anterior to P^2. P^3 alveolus situated immediately posterior to P^2 and no diastema present. Anterior root socket of P^3 is about twice diameter of that of P^2.

Premolar, P^2. P^2 crown low and elongate basally. Cusp points posteriorly and anterior profile slightly convex. Posterior margin of crown distinctly concave. Surface of posterior shelf obscured by an obdurate calcite encrustation. Posterior root about twice as wide mesio-distally as anterior root. Crown length about 6.5 mm; width, 2.5 mm.

P^3. Alveolus only; at least 7.3 mm total length (hypertrophied); anterior root socket about 3.0 mm long and 2.0 mm wide; posterior root socket at least 4.0 mm long, width unknown.

Molar, M^1. Reconstructed from three fragments; heavily worn and thickly coated with calcrete. Crown elongated, transversely narrow; short, distinct precingulum present; deep cleft divides crown into two lobes, shallow but distinct ectoflex. Stylar cusp B about same size as paracone; metacone about half again larger than paracone. Postmetacrista straight, angles slightly lingual to postprotocrista. Preparacrista short, extends transversely to long axis of crown to stylar cusp B. Centrocrista obtuse, essentially parallel to tooth row; stylar cusp D much smaller than metacone, closely situated distolabially and connected to it by low crest with conspicuous groove labial to metacone and mesial to stylar cusp D; small stylar cusp E heavily worn, but faintly visible. Talon short transversely with U-shaped profile. A very small metaconule represented. Cusp heights: metacone > stylar cusp B > stylar cusp D > paracone > protocone.

M^2. Talon only, larger than M^1 talon and more V-shaped. Basin shallow, heavily worn on mesial side; conules absent; crest of base of metacone confluent with postprotocrista.

M^3. Complete crown and roots, reconstructed from four fragments, moderate wear (slight misalignment of fragments due to missing slivers of dentine at contacts). Precingulum short, complete; parastylar spur much shorter than metastylar spur, strong ectoflexus; stylar cusp B connected to paracone by convex, mesially-angled preparacrista; stylar cusp C reduced, but present;

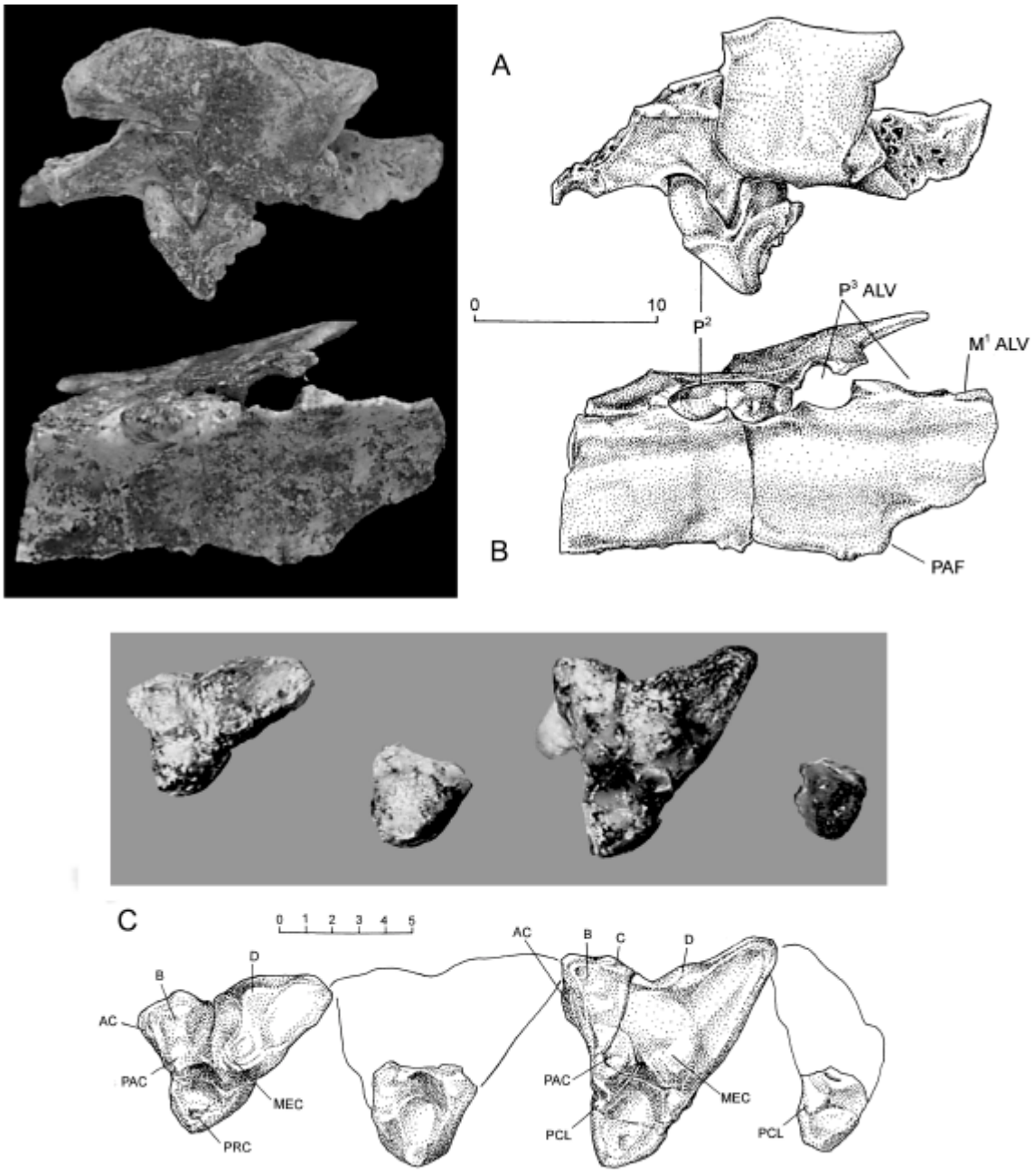

Fig. 6. *Tyarrpecinus rothi* gen. et sp. nov. holotype left maxilla (P98211). Maxillary fragment in **A**, lateral and **B**, occlusal views; **C**, reconstructed molar tooth row (M_{1-4} from left to right) in occlusal view. Scale bars in mm.

low elongated stylar cusp D produces conspicuous labial bulge; distinct, elliptical thickening of enamel in region of stylar cusp E, but no definite cusp structure visible. Metacone much larger and higher than paracone. Angle of centrocrista about 90°; angle between preparacrista and postmetacrista slightly wider than in *Nimbacinus dicksoni* and *Ngamalcinus timmulvaneyi*. Talon narrow, V-shaped, very faint protoconule evident, metaconule absent. Cusp heights: metacone > paracone > stylar cusp D > ?stylar cusp E = stylar cusp B > stylar cusp C > protoconule > protocone.

M⁴. Talon only; greatly reduced compared to M^3; narrow, V-shaped, with low protoconule.

Etymology. Named in honour of Karl Roth for his contributions to the natural history of Central Australia and long career as Custodian of the Alice Springs branch

of the Museums and Art Galleries of the Northern Territory, from which he recently retired.

PHYLOGENY RECONSTRUCTION

Muirhead and Wroe (1998) analysed shared, derived character states amongst five thylacinid genera to reconstruct phylogeny in the family. Of 32 characters analysed, 24 are dental, with the remainder pertaining to the cranium. As a preliminary analysis, the states of the three newly described species plus *Muribacinus gadiyuli* Wroe, 1996, and *Thylacinus megiriani* Murray, 1997, were scored and added to their matrix (Table 2A - necessarily omitting the eight cranial characters) and analysed with Hennig86 version 1.5 (Farris 1988). One of eight equally parsimonious hypotheses selected for discussion purposes is shown as Figure 7A, and the Nelsen consensus tree is shown as Figure 7B.

In Figures 7A and 7B, the previously analysed species branch consecutively in the same order as illustrated in Muirhead and Wroe (1998). Of the new species, *Mutpuracinus archibaldi* aligns with the plesiomorphic *Muribacinus gadiyuli* at the base, and *Tyarrpecinus rothi* branches off after *Ngamalacinus ridei* and *Wabulacinus*.

The emphasis in Muirhead and Wroe (1998) on ordered multistate characters, postulating broad morphoclines for the majority of character states, tends to relegate resulting trees to a hierarchy of structural grades. Notwithstanding, there are some promising synapomorphic states that suggest clade formation within the consecutively branched dendrogram. These include the synapomorphic occurrence of a carnassial notch in the hypocristid of *Badjcinus* and *Ngamalacinus* (Character 28 in Table 2A) and mutual loss of stylar cusp B accompanied by extreme reduction of the stylar shelf in *Wabulacinus ridei* and *Thylacinus macknessi* (Character 11); which, in combination with the strongly morphoclinal expression of metaconid reduction (Characters 18-19) result in the more resolved hypotheses (Fig. 8 based on the character matrix in Table 2B) preferred here.

Muirhead and Wroe (1998) divide the character of metaconid reduction into two sets, Character 18, in which a differential absence of metaconid on M_1 and presence on the other molars is scored autapomorphically among thylacinids for *Badjcinus*, and Character 19 in which the size of metaconids on M_{2-4} is scored as an independant multistate set. The recognition of a unique differential reduction of the metaconid in *Badjcinus* is apparently based on the assumption of uniformly reducing metaconids in *Nimbacinus dicksoni*, as indicated by the D-Site M_2 paratype, QMF16809.

However, *Nimbacinus richi* shows a similar degree of differential metaconid expression to that of *Badjacinus*, in which the cusp is nearly obsolete on M_1, but well-differentiated and large on M_{2-3}, then reduced on M_4. Thus, while the extent of metaconid reduction on M_1 in *Badjacinus* is more advanced than in *Nimbacinus richi*, we do not consider the character of differential expression of the metaconid to be unique to *Badjcinus* (within the Thylacinidae). The states of metaconids in *N. richi* also negate the proposition that the expression

Table 2. Thylacinid character expressions for phylogenetic analysis: **A**, following Muirhead and Wroe (1998), cranial characters 1, 2 and 4-9 omitted; **B**, preferred matrix as discussed in the text. Character definitions for matrices A and B given with Figures 7 and 8 respectively.

A

Characters (Muirhead and Wroe 1998)	**Dasyurid outgroup**	***Muribacinus gadiyuli***	***Mutpuracinus archibaldi***	***Nimbacinus dicksoni***	***Nimbacinus richi***	***Badjcinus turnbulli***	***Ngamalacinus timmulvaneyi***	***Tjarrpecinus rothi***	***Wabulacinus ridei***	***Thylacinus macknessi***	***Thylacinus potens***	***Thylacinus megiriani***	***Thylacinus cynocephalus***
3	0	0	0	1	?	0	1	?	0	?	1	1	1
10	0	1	1	1	?	2	1	2	1	1	2	3	3
11	0	1	1	1	?	2	2	3	3	4	4	4	4
12	0	0	0	0	?	0	0	1	1	0	1	2	2
13	0	0	0	0	?	2	1	2	1	2	2	3	3
14	0	0	0	0	?	1	1	2	2	2	2	2	2
15	0	1	1	1	?	1	1	2	2	2	2	2	2
16	0	0	0	0	?	3	0	1	2	1	1	1	1
17	0	1	1	1	?	1	1	2	2	2	2	2	2
18	0	0	0	0	1	1	0	?	0	0	0	0	0
19	0	1	1	1	1	1	2	?	3	4	4	?	4
20	0	1	1	2	0	1	0	?	4	3	3	?	3
21	0	0	0	0	0	0	1	?	0	0	0	?	0
22	0	0	?	0	0	0	0	?	1	0	0	?	0
23	0	0	?	0	1	0	?	?	?	1	1	?	1
24	0	1	1	1	1	1	2	?	3	4	5	?	5
25	0	0	0	0	1	1	1	?	0	0	0	?	0
26	0	0	0	0	0	0	1	?	0	1	1	?	1
27	0	1	1	1	2	1	2	?	1	3	3	?	3
28	0	0	0	0	0	1	1	?	0	0	0	?	0
29	0	1	1	1	2	1	2	?	2	3	3	?	3
30	0	0	?	1	1	0	?	?	1	1	1	?	1
31	0	?	0	0	0	0	1	?	1	1	1	?	1

B

Characters (this work)													
1	0	0	1	2	2	2	2	?	3	3	4	?	4
2	0	0	0	0	0	1	1	0	0	0	0	0	0
3	0	0	0	0	0	0	0	1	1	1	1	1	1
4	0	0	0	0	0	0	0	0	1	1	0	0	0
5	0	0	0	0	0	0	0	1	0	0	1	1	1
6	0	0	0	0	0	0	0	0	1	1	0	0	0
7	0	0	0	0	0	0	0	0	0	0	0	1	1
8	0	0	0	0	0	0	0	1	1	1	1	1	1

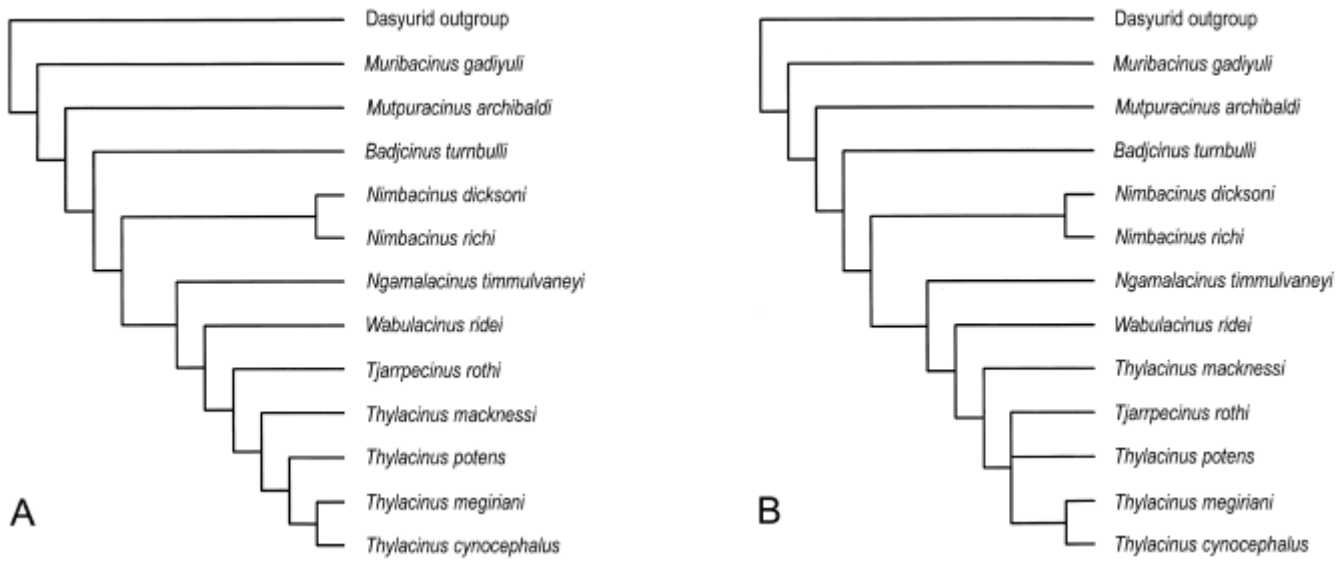

Fig. 7. A, one of eight equally parsimonious trees depicting thylacinid phylogeny using character matrix after Muirhead and Wroe (1998) (see Table 2A of this work); **B**, Nelsen consensus of the eight equally parsimonious trees (Consistency Index = 0.73; Retention Index = 0.85: Hennig86 version 1.5 (Farris 1988)). *Abridged definitions of character expressions* (see Muirhead and Wroe 1998 for details). **3**, infraorbital foramen: 0, not bounded by jugal; 1 bounded by jugal. **10**, size of paracone: 0, equivocal plesiomorphic state; 1, slight reduction; 2, significant reduction; 3, extreme reduction. **11**, stylar cusp B: 0, well developed; 1, slight reduction; 2, greater reduction; 3, more reduced yet; dramatically reduced [Muirhead and Wroe (1998) include the stylar shelf and stylar cusp D in this morphocline: actual loss or extreme reduction of stylar cusp B in thylacinids is confined to *Thylacinus macknessi* and *Wabulacinus ridei* (Muirhead 1992, 1997).] **12**, anterior cingulum: 0, complete; 1, incomplete. **13**, protocone and conules: 0, well developed; 1, slightly reduced; 2, significant reduction; 3, conules lost. **14**, length postmetacrista: 0, as in dasyurids; 1, slight elongation. **15**, angle centrocrista: 0, acute; 1, more obtuse than in dasyurids; 2, colinear. **16**, direction of preparacrista: 0, perpendicular; 1, slightly oblique; 2, parallel to long axis; 3, directly anterior to paracone. **17**, angles preparacrista and postmetacrista: 0, narrow; 1, slightly widening; 2, wider yet. **18**, size of metaconid in M_1 relative to M_{2-4}: 0, uniform reduction; 1, variably absent on M_1, present M_{2-4}; **19**, size metaconid M_{2-4}: 0, plesiomorphic condition; 1, some reduction; 2 more reduced; nearly lost; 4, lost. **20**, size entoconid: 0, large; 1, slight reduction; 2, greater reduction; 3, very reduced; 4, absent. **21**, morphology entoconid: 0, plesiomorphic condition; 1, laterally compressed. **22**, diastema P1-2: 0, present; 1, absent. **23**, diastema P2-3: 0, present; 1, absent. **24**, hypoconulid / hypoconulid notch: 0, present; 1, slightly diminished; 2, obvious reduction; 3, more reduced yet; 4, extremely reduced; 5, notch absent. **25**, posterior cingulid and hypocristid: 0, separated; 1, joined. **26**, cristid obliqua carnassial notch: 0, absent; 1, present. **27**, angle hypocristid: 0, parallel to transverse axis of dentary; 1, moderate angle; 2, intermediate; 3, pronounced. **28**, carnassial notch in hypocristid: 0, absent; 1, present. **29**, termination of cristid obliqua: 0, low; 1, higher; 2, stronger, higher; 3, principle posterior shearing crest. **30-31**, size P3, two pathways: 00, 01, plesiomorphic; 10 apomorphic [see Muirhead and Wroe (1998) for explanation.] **32**, length M_4: 0, shorter than M_3; longer than M_3.

gradient of the metaconid along the molar row is typically uniform in thylacinids. In any case, the differential reduction of metaconids in *Badjcinus turnbulli, Nimbacinus richi* and *Ngamalcinus timmulvaneyi* may be the rule rather than the exception, and as such, the basic similarity of the differentially reduced states of the metaconids in these species is probably more meaningful for thylacinid phylogeny than the autapomorphic absence of a metaconid on M^1 in *Badjcinus*.

The inclusion of *Muribacinus gadiyuli* and *Mutpuracinus archibaldi* present a fairly complete picture of the morphocline for metaconid reduction in thylacinids: *Muribacinus gadiylui* shows gradual posterior enlargement of the metaconids (0); *Mutpuracinus archibaldi* shows a slight reduction in the size of M_4 metaconid (1), (M_{1-2} unknown); *Ngamalacinus timmulvaneyi* shows marked reduction of metaconid on M_1 and M_4; *Nimbacinus richi* shows further reduction of metaconid on M_1 with no further reduction on M_4 than in the former species, and *Badjcinus turnbulli* shows complete loss of metaconid on M_1 with no further reduction on M_4 than in the former species (2); while the metaconid is nearly obsolete on all molars of *Wabulacinus ridei* and *Thylacinus macknessi* (3) and lost on all other species of *Thylacinus* (4).

Resolution of clade formation is obscured by the establishment of several interrelated morphoclines (widened angle of preparacrista and postmetacrista, straightened centrocrista, elongation of postmetacrista, stylar shelf and cusp reduction) expressing progressive states of carnassialisation in the Thylacinidae. These overwhelm the otherwise compelling evidence for at least two parallel trends in development of longer shearing crests while simultaneously suppressing the relatively few synapomorphic states that might otherwise

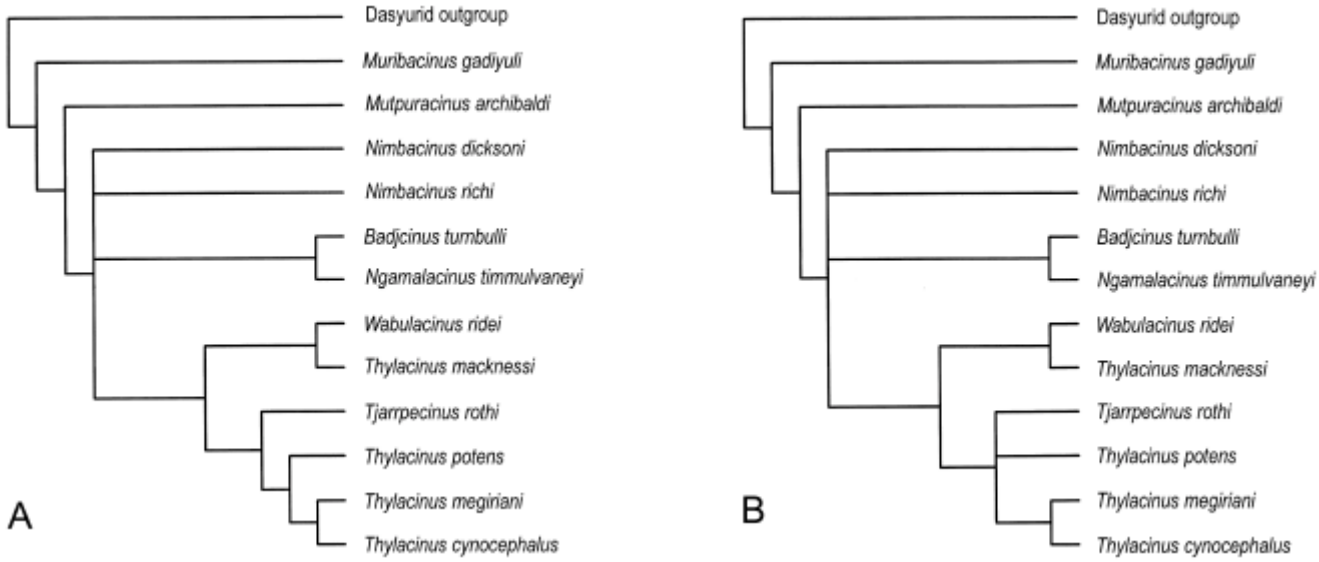

Fig. 8. Dendrograms (**A**, more, and **B**, less, resolved) depicting preferred hypotheses of thylacinid phylogeny based on a restricted suite of characters (Table 2B) which do not include the autapomorphous and discontinuous characters of Table 2A. (Hennig86 version 1.5 (Farris 1988); 2 equally parsimonious trees; Consistency Index = 1.0; Retention Index = 1.0). *Definitions of character expression.* **1**, pattern of metaconid reduction: 0, slight, uniform; 1, slight M_4; 2, differential, marked on M_1, slight M_4; 3, near obsolescence on all molars; 4, entirely lost on all molars. **2**, carnassial notch in hypocristid: 0, absent; 1, present. **3**, elongation of postvallum, shearing surfaces: 0, slight; 1, significant. **4**, stylocone B: 0, present; 1, extremely reduced or lost. **5**, paracone reduction / hypertrophy of metacone: 0, slight – moderate; 1, conspicuous. **6**, ectoflexus: 0, strong expression; 1, weak expression. **7**, precingulum: 0, present, strong; 1, reduced – absent. **8**, entoconid: 0, distinct; 1, reduced – absent.

have been recognised by the algorithm. While it is true that there is a general trend towards increased carnassialization signalled among these genera, and that the structural changes that characterise these trends are essentially indistinguishable (the possible exception being *T. macknessi* - Muirhead 1992: 72), the disjunct nature of the character combinations indicate that the similarities in the states of carnassialization between *Thylacinus macknessi*, *Wabulacinus ridei* and the comparably derived species of *Thylacinus* are phylogenetically uninformative homoplasy.

As Muirhead (1992, 1997) and Muirhead and Gillespie (1995) point out, both *Wabulacinus ridei* and *Thylacinus macknessi* show progressive states of carnassialization (loss of stylar cusps, extreme reduction-loss of stylar shelf, lengthening, straightening of crests) in combination with several autapomorphies and retained plesiomorphies (relatively unreduced paracones). Whereas in *Tyarrpecinus* and other members of *Thylacinus*, carnassialization has proceeded in conjunction with plesiomorphous retention of the stylar shelf, stylar cusps and apomorphous reduction of paracone and/or enlargement of metacone. In other words, the crown genera share an ancestor with states close to *Nimbacinus*, rather than, as the Muirhead and Wroe (1998) cladogram implies, direct, successive sister relationships with *Wabulacinus ridei* and *Thylacinus macknessi*.

Tyarrpecinus rothi is therefore considered to represent the plesiomorphic sister-taxon of the *Thylacinus* clade (*T. potens* + *T. megiriani* + *T. cynocephalus*, but not *T. macknessi*) (Fig. 8A,B), as it is too derived (more reduced M^1 paracone and precingulum) to have given rise to *Thylacinus macknessi* and probably *Wabulacinus ridei* (greater paracone reduction on M^1) while lacking highly derived states of stylar cusp and stylar shelf reduction/loss of the *Thylacinus* clade. *Tyarrpecinus rothi* shows incipient to moderate development of *Thylacinus*-like states in the considerable reduction of the parastylar spur, reduction of the precingulum, elongation of the postmetacrista; mesial obliquity of the preparacrista, reduction of the paracone, extreme reduction to loss of conules and reduction of the trigone basin on M^3. Resemblance to particular species of *Thylacinus* are evident, such as strong ectoflex present in *T. potens* and *T. megiriani* M^3. There is also the question of the expression of a tiny stylar cusp E which appears to be present in the form of an elliptical thickening of the stylar crest of M^3 in both *Tyarrpecinus* and *Thylacinus megiriani* (Murray 1997). Although Muirhead and Wroe (1998) have concluded that the tiny stylar cusp on the M^3 of *Thylacinus cynocephalus* represents a distally-shifted stylar cusp D, we prefer to wait for additional data.

Other than some minor shifts in emphasis on some of the character states, the new data present no significant points of disagreement with recently proposed hypotheses of thylacinid phylogeny (Muirhead

and Archer 1990, Muirhead 1992, Muirhead and Gillespie 1995, Wroe 1996, Murray 1997, Muirhead and Wroe 1998). However, the problem of association of the upper and lower molars of *Nimbacinus dicksoni* creates an ambiguity in character states of a pivotal group. The D-Site M_2 (QMF16809) has a much narrower paraconid and much smaller metaconid than the equivalent molar of the Bullock Creek LF *Nimbacinus* (P9612-4), so we are certain that it represents a different taxon, probably another genus, in concert with the current level of systematic discrimination. However, the Bullock Creek LF specimens (P85553-3 and P9612-4) are sufficiently close to the holotype M_2 (QMF16802) to indicate a species-level distinction, and accordingly, we have inferred that the unknown M_{2-3} of *N. dicksoni* are as similar to *N. richi* as is the M_1.

Although poorly represented, the *Tyarrpecinus rothi* morphotype is sufficiently generalised to represent the structural stage that may have given rise to all *Thylacinus* species except *T. macknessi*, and perhaps to *Wabulacinus ridei*. On the basis of present information, *Thylacinus macknessi* branched off from a less derived form than *Tyarrpecinus*. Taking the few synapomorphies between *Wabulacinus* and *Thylacinus macknessi* at face value, they become, more or less by default, sister taxa in a minor clade (Fig. 8A,B) characterised by progressive, predominantly homoplasious carnassialization. Muirhead and Archer's (1990) observations on some strong similarities between *N. dicksoni* and *T. potens* Woodburne, 1967, become more pertinent here, because, as they suggest, the well-developed ectoflexus in *N. dicksoni* may constitute a synapomorphic condition. With the additions of *Mutpuracinus archibaldi*, *Tyarrpecinus rothi* and *Thylacinus megiriani*, all of which display strong ectoflexus on M^3, we are inclined to favour the interpretation of a symplesiomorphy retained in a conservative lineage culminating with the genus *Thylacinus*.

STRATIGRAPHIC PALAEONTOLOGY AND BIOCHRONOLOGY

The newly described Bullock Creek and Alcoota LF species brings the total number of ?late Oligocene and Miocene thylacinids to 11 species in eight genera, all but *Nimbacinus* and *Thylacinus* being monospecific. No species are represented by abundant material, and thylacinids are presently of minimal use in intraformational biocorrelation and of no use in intracontinental correlation (Table 3). Even at the generic level, a high degree of faunal regionalism is indicated, which follows the general pattern observed by Rich (1991) for the Australian mid Tertiary vertebrate record.

There is stratigraphic evidence of sympatry for: *Mutpuracinus archibaldi* + *Nimbacinus richi* ('Top Site', Camfield Beds); *Ngamalacinus timmulvaneyi* + *Wabulacinus ridei* ('Camel Sputum Site', Carl Creek Limestone); *Thylacinus macknessi* + *Muribacinus gadiyuli* ('Gag Site', Carl Creek Limestone) and *Thylacinus potens* + *Tyarrpecinus rothi* (Waite Formation - two excavation sites, 'Main Pit' and 'Paine Quarry', sampling the Alcoota LF horizon) (Table 4). Although the 'Top Site' (Camfield Beds) assemblage is drawn from several lithofacies (Murray and Megirian 1992), and therefore possibly different beds, P9215-4 (*Nimbacinus richi*) and P9215-5 (*Mutpuracinus archibaldi*) were found lying one upon the other in the same block of limestone.

Table 3. Stratigraphic distribution of ?late Oligocene and Miocene species of Thylacinidae, and biocorrelation of fossil assemblages.

Formation (geographic location)	Local Fauna	Site / Quarry	Species
Waite Formation (Alcoota)	Ongeva	South Quarry	*Thylacinus megiriani*
	Alcoota	Paine Quarry	*Thylacinus potens*
	Alcoota	Main Pit	*Tyarrpecinus rothi*
Camfield Beds (Bullock Creek)	Bullock Creek	Top Site	*Mutpuracinus archibaldi*
	Bullock Creek	Top Site	*Nimbacinus richi*
	Bullock Creek	Blast Site	*Nimbacinus richi*
Carl Creek Limestone (Riversleigh)		Camel Sputum	*Ngamalacinus timmulvaneyi*
		Inabeyance	*Ngamalacinus timmulvaneyi*
		Camel Sputum	*Wabulacinus ridei*
		D-Site	*Nimbacinus dicksoni*
		Henks Hollow	*Nimbacinus dicksoni*
		Gag	*Muribacinus gadiyuli*
		Gag	*Thylacinus macknessi*
		Nevilles Garden	*Thylacinus macknessi*
		Mikes Menagerie	*Thylacinus macknessi*
		White Hunter	*Badjcinus turnbulli*

Table 4. Stratigraphic evidence of sympatry amongst Miocene thylacinids.

Formation	Local Fauna	Site	Species
Waite Formation	Ongeva	South Quarry	*Thylacinus megiriani*
	Alcoota	Paine Quarry	*Thylacinus potens*
		Main Pit	*Tyarrpecinus rothi*
Camfield Beds	Bullock Creek	Top Site	*Mutpuracinus archibaldi*
		Top Site	*Nimbacinus richi*
		Blast Site	*Nimbacinus richi*
Carl Creek Limestone		Camel Sputum	*Ngamalacinus timmulvaneyi*
		Camel Sputum	*Wabulacinus ridei*
		White Hunter	*Badjcinus turnbulli*
		Gag	*Muribacinus gadiyuli*
		Gag	*Thylacinus macknessi*
		Inabeyance	*Ngamalicinus timmulvaneyi*
		Henks Hollow	*Nimbacinus dicksoni*
		D-Site	*Nimbacinus dicksoni*
		Mikes Menagerie	*Thylacinus macknessi*
		Nevilles Garden	*Thylacinus macknessi*

The only biostratigraphic evidence of temporal succession amongst thylacinids comes from superposition in the Waite Formation of *Thylacinus megiriani* (Ongeva LF) over *Thylacinus potens* and *Tyarrpecinus rothi* (Alcoota LF) (Murray *et al.* 1993; Megirian *et al.* 1996; Murray 1997; Megirian 2000), but a broader interpretive perspective is provided by zygomaturine stage-of-evolution biochronology (Woodburne *et al.* 1985; Megirian 1994; Murray *et al.* 2000) (Table 5). The as yet un-named species of *Neohelos* from the Camfield Beds and Carl Creek Limestone 'Gag' and 'Henks Hollow' sites (Murray *et al.* 2000) is here identified as '*Neohelos* sp. nov.'. The following conclusions can be drawn from Table 5.

1. The apparent contemporaneity of *Nimbacinus richi* (Camfield Beds) and *Nimbacinus dicksoni* (Carl Creek Limestone) in *Neohelos* sp. nov. time suggests that these were allopatric sibling species.

2. *Thylacinus macknessi* lived at Riversleigh from *Neohelos tirarensis* to *Neohelos* sp. nov. time, which Murray *et al.* (2000) suggest may have spanned the latest Oligocene to mid Miocene. If 'D-Site' *Nimbacinus dicksoni* is actually conspecific with 'Henks Hollow' *N. dicksoni* as proposed by Muirhead and Archer (1990), then this taxon may have had a similar temporal range. Alternatively, the 'D-Site' *Nimbacinus* material may represent a different species, as discussed in the Systematics section above, which could conceivably represent the ancestor of one or both of *Nimbacinus dicksoni* and *N. richi*.

3. Five species of thylacinid may have co-existed at Riversleigh during *N. tirarensis* time, supporting the conclusions of Muirhead (1997), Muirhead and Wroe (1998) and of this study that a major phylogenetic radiation of thylacinids occurred before the ?late Oligocene (= pre *N. tirarensis* time).

4. No potential ancestor–descendent relationships have been identified amongst the 11 known Miocene thylacinid species: *Mutpuracinus archibaldi* is identified above as having structural states that may reflect the ancestral conditions giving rise to *Nimbacinus dicksoni*, but a phyletic succession from *M. archibaldi* to *N. dicksoni* is not consistent with biochronological indications in that *Mutpuracinus archibaldi* post-dates the earliest record of *Nimbacinus dicksoni*.

Estimating changes in thylacinid diversity through the Miocene is problematic due to different taphonomic processes at the very few known fossil-producing localities. Remains of small taxa are rare in the ephemeral channel and overbank deposits of the Waite Formation, and small terrestrial animals are sparse in the billabong and channel deposits of the Camfield Beds (Murray and Megirian 1992). Persistent sampling over many years produced the three new species reported here. In contrast, the small-scale cave-entrance/perched springline, fluvial tufa and associated pond deposits of the *N. tirarensis* biochron of the Carl Creek Limestone are noted for their preservation of small and medium-sized animals (e.g. Archer *et al.* 1989, 1991; Megirian 1992, 1997). The apparent decline in diversity in the Carl Creek Limestone from five species during *Neohelos tirarensis* time to two species during *Neohelos* sp. nov. time, with no species reported yet from apparently younger zygomaturine biochrons, may also reflect preservational and sampling biases.

The association of quite highly advanced and very conservative forms in the Carl Creek Limestone during *N. tirarensis* time (e.g. *Thylacinus macknessi* +

Table 5. A, thylacinid biochronology in terms of zygomaturine stage-of-evolution (Murray et al. 2000): *Neohelos tirarensis* stage ≡ latest Oligocene / early Miocene; *Neohelos* sp. nov. stage ≡ middle Miocene; *Kolopsis torus* stage ≡ late Miocene; *K. yperus* stage ≡ latest Miocene. * No *Neohelos* has been described from Carl Creek Limestone White Hunter Site, which is here tied in by simple marsupial biocorrelation, **B**, using burramyids (Brammall and Archer 1997), macropodids (Cooke 1997: table 1), phascolarctids (Black and Archer 1997) and the diprotodontoid *Bematherium angulum* (Black 1997: fig.1). White Hunter clusters with sites containing *N. tirarensis*, using Bray and Curtis agglomeration analysis and flexible UPGMA (Un-weighted Pair Group Method, Arithmetic average) algorithms in PATN (Belbin 1994).

A

Formation	**Local Fauna**	**Site**	**Thylacinid species**	**Zygomaturine stage-of-evolution** (Murray *et al.* 2000)
Waite Formation	Ongeva	South Quarry	*Thylacinus megiriani*	*Kolopsis yperus* (+ *Kolopsis torus*)
-unconformity-				
Waite Formation	Alcoota	Paine Quarry	*Thylacinus potens*	*Kolopsis torus*
Waite Formation	Alcoota	Main Pit	*Tyarrpecinus rothi*	*Kolopsis torus*
Camfield Beds	Bullock Creek	Top	*Mutpuracinus archibaldi*	*Neohelos* sp. nov.
Camfield Beds	Bullock Creek	Top	*Nimbacinus richi*	*Neohelos* sp. nov.
Camfield Beds	Bullock Creek	Blast	*Nimbacinus richi*	*Neohelos* sp. nov.
Carl Creek Limestone		Gag	*Muribacinus gadiyuli*	*Neohelos* sp. nov.
Carl Creek Limestone		Gag	*Thylacinus macknessi*	*Neohelos* sp. nov.
Carl Creek Limestone		Henks Hollow	*Nimbacinus dicksoni*	*Neohelos* sp. nov.
Carl Creek Limestone		Camel Sputum	*Ngamalacinus timmulvaneyi*	*Neohelos tirarensis*
Carl Creek Limestone		Camel Sputum	*Wabulacinus ridei*	*Neohelos tirarensis*
Carl Creek Limestone		Inabeyance	*Ngamalacinus timmulvaneyi*	*Neohelos tirarensis*
Carl Creek Limestone		D-Site	*Nimbacinus dicksoni*	*Neohelos tirarensis*
Carl Creek Limestone		Mikes Menagerie	*Thylacinus macknessi*	*Neohelos tirarensis*
Carl Creek Limestone		Nevilles Garden	*Thylacinus macknessi*	*Neohelos tirarensis*
Carl Creek Limestone		White Hunter	*Badjcinus turnbulli*	*(Neohelos tirarensis)**

B

Site	***Burramys brutyi***	***Bulungamaya delicata***	***Wabularoo naughtoni***	***Ganawamaya* sp2**	***Balbaroo gregoriensis***	***Nambaroo* sp5**	***Nowidgee matrix***	***Litokoala kanunkaensis***	***Nimiokoala greystanesi***	***Bematherium angulum***	***Neohelos* sp. nov.**	***Neohelos tirarensis***
Gag	1	1		1				1			1	
Henks Hollow	1			1				1			1	
Mikes Menagerie			1									1
Camel Sputum	1	1	1		1	1	1		1			1
Nevilles Garden	1	1	1		1	1			1			1
Inabeyance	1				1				1			1
D-Site		1	1							1		1
White Hunter	1		1				1			1		*

Muribacinus gadiyuli) reflects the extent of independent (parallel) evolution of lineages which emerged in the Paleogene, including the crown group comprising the Waite Formation species and culminating in the recently extinct 'Tasmanian wolf', *T. cynocephalus*. It appears, from absence in the later fossil record, that by the late Miocene (*Kolopsis torus* time), all the conservative lineages as well as the quite advanced *Thylacinus macknessi* + *Wabulacinus ridei* clade, had become extinct, but the pattern of succession is not clear.

REFERENCES

Archer, M. 1978. The nature of the molar-premolar boundary in marsupials and interpretation of the homology of marsupial cheekteeth. *Memoirs of the Queensland Museum* **18**: 157-164.

Archer, M. 1982. A review of Miocene thylacinids (Thylacinidae: Marsupialia), the phylogenetic position of the Thylacinidae and the problem of apriorisms in character analysis. In: Archer, M. (ed.) *Carnivorous marsupials*. Pp. 445-476. Royal Zoological Society of New South Wales: Sydney, Australia.

Archer, M., Godthelp, H., Hand, S.J. and Megirian D. 1989. Fossil mammals of Riversleigh, northwestern Queensland: preliminary overview of biostratigraphy, correlation and environmental change. *Australian Zoologist* **25**(2): 29–65.

Archer, M., Hand S.J. and Godthelp, H. 1991. *Riversleigh. The story of animals in ancient rainforests of inland Australia*. Reed Books Pty Ltd: Sydney, Australia.

Belbin, L. 1994. PATN, pattern analysis package users guide. CSIRO Division of Wildlife and Ecology, Lyneham ACT, Australia.

Black, K. 1997. Diversity and biostratigraphy of the Diprotodontoidea of Riversleigh, northwestern Queensland. *Memoirs of the Queensland Museum* **41**(2): 187-192.

Black, K. and Archer, M. 1997. *Nimiokoala* gen nov. (Marsupialia, Phascolarctidae) from Riversleigh, northwestern Queensland, with a revision of *Litokoala*. *Memoirs of the Queensland Museum* **41**(2): 209-228.

Bonaparte, C.L.J.L. 1838. Synopsis vertebratorium systematis. *Nuovi Annual, Science and Nature, Bologna* **2**: 105-133.

Brammall, J. and Archer, M. 1997. A new Oligocene-Miocene species of *Burramys* (Marsupialia, Burramyidae) from Riversleigh, northwestern Queensland. *Memoirs of the Queensland Museum* **41**(2): 247-268.

Cooke, B.N. 1997. Biostratigraphic implications of fossil kangaroos at Riversleigh, northwestern Queensland. *Memoirs of the Queensland Museum* **41**(2): 295-302.

Dawson, L. 1982. Taxonomic status of fossil thylacines (*Thylacinus*, Thylacinidae, Marsupialia) from late Quaternary deposits in eastern Australia. In: Archer, M. (ed.) *Carnivorous marsupials*. Pp 445-476. Royal Zoological Society of New South Wales: Sydney, Australia.

Farris, J.S. 1988. Hennig86. Version 1.5. Port Jefferson Station: New York.

Flower, W. 1869. Remarks on the homologies and notation of teeth in the Marsupialia. *Journal of Anatomy and Physiology* **3**: 262-278.

Gill, T. 1872. Arrangement of families of mammals with analytical tables. *Smithsonian Miscellaneous Collection* **2**: 1-98.

Goldfuss, G. 1820. *Handbuch der Zoologie.* Abteilung II. J. L. Schrag: Nuremburg.

Henderson, J. and Dobson, V. 1994. *Eastern and Central Arrente to English dictionary*. IAD Press: Alice Springs, Australia.

Luckett, P. 1993. An ontogenetic assessment in dental homologies in the therian mammals. In: Szalay, F., Novacek, M., and McKenna, M. (eds) *Mammal phylogeny: Mesozoic differentiation, multituberculates, monotremes, early therians, and marsupials.* Pp 182-204. Springer-Verlag: New York.

Megirian, D. 1992. Interpretation of the Miocene Carl Creek Limestone, northwestern Queensland. *The Beagle. Records of the Northern Territory Museum of Arts and Sciences* **9**(1): 219–248.

Megirian, D. 1994. Approaches to marsupial biochronology in Australia and New Guinea. *Alcheringa* **18**: 259-274.

Megirian, D. 1997. The geology of the Carl Creek Limestone. Unpublished PhD thesis, Flinders University of South Australia, Adelaide.

Megirian, D. 2000. Report on shallow augering at the MAGNT Alcoota Fossil Reserve, June and August, 1998. Museums and Art Galleries of the Northern Territory Research Report 7.

Megirian, D., Murray, P.F. and Wells, R.T. 1996. The late Miocene Ongeva Local Fauna of central Australia, *The Beagle, Records of the Museums and Art Galleries of the Northern Territory* **13**: 9-38.

Muirhead, J. 1992. A specialised thylacinid, *Thylacinus macknessi,* (Marsupialia: Thylacinidae) from Miocene deposits of Riversleigh, northwestern Queensland. *Australian Mammalogy* **15**: 67-76.

Muirhead, J. 1997. Two early Miocene thylacines from Riversleigh, northwestern Queensland. *Memoirs of the Queensland Museum* **41**(2):367-377.

Muirhead, J. and Archer, M. 1990. *Nimbacinus dicksoni*, a plesiomorphic thylacine (Marsupialia: Thylacindae) from Tertiary deposits of Queensland and the Northern Territory. *Memoirs of the Queensland Museum* **28**(1): 203-221.

Muirhead, J. and Gillespie, A. 1995. Additional parts of the type specimen of *Thylacinus macknessi* (Marsupialia: Thylacinidae) from Miocene deposits of Riversleigh, northwestern Queensland. *Australian Mammalogy* **18**: 55-60.

Muirhead, J. and Wroe, S. 1998. A new genus and species, *Badjcinus turnbulli* (Thylacinidae: Marsupialia) from the late Oligocene of Riversleigh, northern Australia, and an investigation of thylacinid phylogeny. *Journal of Vertebrate Paleontology* **18**(3): 612-626.

Murray, P.F. and Megirian, D. 1992. Continuity and contrast in middle and late Miocene vertebrate communities from the Northern Territory. *The Beagle, Records of the Northern Territory Museum of Arts and Sciences* **9**(1):195-218.

Murray, P.F. 1997. *Thylacinus megiriani*, a new species of thylacine (Marsupialia: Thylacinidae) from the Ongeva Local Fauna of central Australia. *Records of the South Australian Museum* **30**(1): 43-61.

Murray, P.F., Megirian, D. and Wells, R.T. 1993. *Kolopsis yperus* sp. nov. (Zygomaturinae, Marsupialia) from the Ongeva Local Fauna: new evidence for the age of the Alcoota fossil beds of central Australia. *The Beagle, Records of the Northern Territory Museum of Arts and Sciences* **10**(1):155-172

Murray, P.F., Megirian, D., Rich, T.H., Plane, M., Black, K., Archer, M., Hand, S. and Vickers-Rich, P. 2000. Morphology, systematics and evolution of the marsupial genus *Neohelos* Stirton (Diprotodontidae, Zygomaturinae). Museums and Art Galleries of the Northern Territory Research Report 6.

Rich, T.H. 1991. Monotremes, placentals, and marsupials: their record in Australia and its biases. In: Vickers-Rich, P., Monaghan, J.M., Baird, R.F. and Rich, T.H. (eds) *Vertebrate palaeontology of Australasia*. Pp 893-1069. Pioneer Design Studio and Monash University Publications Committee: Melbourne, Australia.

Tindale, N.B. 1974. *Aboriginal tribes of Australia.* University of California Press: Berkeley.

Woodburne, M.O. 1967. The Alcoota Fauna, central Australia. An integrated palaeontological and geological study. *Bureau of Mineral Resources Bulletin* **87**: 1-187.

Woodburne, M.O., Tedford, R.H., Archer, M., Turnbull, W.D., Plane, M.D., and Lundelius Jr, E.L. 1985. Biochronology of the continental mammal record of Australia and New Guinea. *Special Publication of the South Australian Department of Mines and Energy* **5**:347-363.

Wroe, S. 1996. *Muribacinus gadiyuli* (Thylacinidae: Marsupialia), a very plesiomorphic thylacinid from the Miocene of Riversleigh, northwestern Queensland, and the problem of paraphyly for the Dasyuridae (Marsupialia). *Journal of Paleontology* **70**(6): 1032-1044.

Accepted 21 November 2000